Theriogenology 140 (2019) 188–200

Contents lists available at ScienceDirect

Theriogenology

journal homepage: www.theriojournal.com

A new thiocyanoacetamide (2-cyano-2-p-nitrophenyl-N-benzylthioamide) reduces doxorubicin-induced *in vitro* toxicity in Sertoli cells by decreasing apoptosis and autophagy

Marwa Boussada [a, 1], Tânia R. Dias [b, c, d, 1], Luís Crisóstomo [b, f], Azaiez B. Akacha [e], Ridha B. Ali [a], Michèle V. El May [a], Marco G. Alves [b, *], Pedro F. Oliveira [b, f, g, **]

[a] *Laboratory of Histology and Embryology, Research Unit N°17/ES/13, Faculty of Medicine of Tunis, University of Tunis El Manar (UTM), Jabbari Jebel Lakhdar Street 15, 1007, Tunis, Tunisia*
[b] *Department of Microscopy, Laboratory of Cell Biology, Unit for Multidisciplinary Research in Biomedicine (UMIB), Institute of Biomedical Sciences Abel Salazar (ICBAS), University of Porto, R. de Jorge Viterbo Ferreira 228, 4050-013, Porto, Portugal*
[c] *Universidade da Beira Interior, R. Marquês d'Ávila e Bolama, 6201-001, Covilhã, Portugal*
[d] *LAQV/REQUIMTE - Laboratory of Bromatology and Hydrology, Faculty of Pharmacy, University of Porto, 4050-313, Porto, Portugal*
[e] *Laboratory of Organic Synthesis and Heterocyclic Chemistry Department, Faculty of Sciences of Tunis, University of Tunis El Manar, 2092, Tunis, Tunisia*
[f] *i3S, Instituto de Investigação e Inovação em Saúde, Universidade do Porto, R. Alfredo Allen, 4200-135, Porto, Portugal*
[g] *Department of Genetics, Faculty of Medicine, University of Porto, 4050-313 Porto, Portugal*

ARTICLE INFO

Article history:
Received 20 November 2018
Received in revised form
19 July 2019
Accepted 25 August 2019
Available online 26 August 2019

Keywords:
Apoptosis
Doxorubicin
Mitochondria
Necrosis
Reactive oxygen species
Sertoli cells

ABSTRACT

Despite conflicting data on doxorubicin (DOX) reproductive toxicity, its chemotherapeutic potential sustains its use to treat different types of cancer. This work was designed to study the protective effect of a newly synthesized thiocyanoacetamide (TA), in comparison with selenium (Se), against doxorubicin-induced *in vitro* toxicity in rat Sertoli cells (SCs). DOX was administered alone or in combination with Se or TA. The possible protective role of increased concentrations of TA (0.25, 0.5 and 1 mM) or Se (12, 25 and 50 μM) on SCs was tested against 1 μM of DOX. From this screening, only the least toxic doses of TA and Se were used for further analysis. DOX cytotoxicity, as well as its impact on SCs viability, mitochondrial membrane potential ($\Delta\Psi_m$), oxidative stress biomarkers, apoptosis and autophagy were assessed. Our results showed that DOX exerted its cytotoxic effect through a significant increase in cell death. DOX-mediated cell death was not related to autophagy nor to an overproduction of reactive oxygen species. It was rather due to apoptosis, as shown by the increased number of apoptotic cells and increased activity of caspase-3, or due to necrosis, as shown by the increase in lactate dehydrogenase (LDH) extracellular activity. Still, Bax and Bcl-2 protein expression levels, as well as $\Delta\Psi_m$ were not altered by the different treatments. Some individual doses of Se or TA induced a significant toxicity in SCs, however, when combined with DOX, there was a decrease in cell death, LDH extracellular activity, number of apoptotic cells and caspase-3 activity. Overall, our results indicate that DOX-mediated apoptosis in cultured SCs can possibly be averted through its association with specific doses of Se or TA. Nevertheless, TA showed a higher efficiency than Se in reducing DOX-induced toxicity in SCs by decreasing not only apoptosis, but also necrosis and autophagy.

* Corresponding author. Department of Microscopy, Laboratory of Cell Biology, Institute of Biomedical Sciences Abel Salazar (ICBAS), University of Porto, Rua de Jorge Viterbo Ferreira 228, 4050-313, Porto, Portugal.
** Corresponding author. Department of Microscopy, Laboratory of Cell Biology, Institute of Biomedical Sciences Abel Salazar (ICBAS), University of Porto, Rua de Jorge Viterbo Ferreira 228, 4050-313, Porto, Portugal.
E-mail addresses: boussadamarwa@gmail.com (M. Boussada), taniadias89@gmail.com (T.R. Dias), luis.d.m.crisostomo@gmail.com (L. Crisóstomo), azaiezbenakacha@yahoo.fr (A.B. Akacha), ridhabenali9@gmail.com (R.B. Ali), elmay_michele@yahoo.fr (M.V. El May), alvesmarc@gmail.com (M.G. Alves), pfobox@gmail.com (P.F. Oliveira).
[1] both authors contributed equally.

https://doi.org/10.1016/j.theriogenology.2019.08.030
0093-691X/

1. Introduction

In many countries, cancer is responsible for more than a quarter of all deaths. The global impact of cancer reached a high socio-economic burden [1]. In fact, approximately 14.1 million people are expected to develop a malignant disease annually. Recent developments in combined chemotherapy and early detection of malignancy have enhanced patient's survival rates. Nevertheless, about two-thirds of the patients need additional treatment for the side effects promoted by the chemotherapeutic agents, including cardiovascular abnormalities, neurocognitive damages and gonadotoxicity [2]. This resulted in a wide consciousness regarding the short and the long-term impact of many chemotherapeutic drugs. The main problem of these drugs is the low selectivity for tumor cells, therefore the treatment will also affect healthy regenerating cells [3].

The dynamic process of spermatogenesis makes the testicular tissue highly sensitive to side-effects caused by chemotherapeutic drugs, leading to temporary or permanent infertility [4]. Among all chemotherapy agents, doxorubicin (DOX), a non-selective [5] class I antibiotic anthracycline [6] is considered by the Food and Drug Administration (FDA) as one of the most potent antineoplasic agents [7]. However, several studies highlighted the negative impact of DOX therapy in male fertility. The widely recognized DOX potential to destroy highly proliferating abnormal cells and to limit tumor progression is accompanied by a high morbidity in normal cells. DOX has the ability to intercalate DNA [7] and interfere with different DNA-binding enzymes, resulting in DNA damage. Consequently, DNA repair fails and cell cycle is arrested, which triggers cell death by apoptosis [8] and necrosis through genetic instability [9]. Recently, it was reported that DOX also promotes the formation of autophagic vacuoles [10]. Additionally, DOX is considered a mitochondrial toxin as it causes a genotoxic stress that leads to mitochondrial dysfunction [11].

During the last decades, a plethora of chemicals have been tested for their ability to inhibit or prevent DOX undesired toxicity to healthy cells. The trace element selenium (Se) is an important factor for human body homeostasis. Se deficiency has been correlated with the loss of vital functions and increased risk for the onset of several diseases, including cancer and infertility [12]. Se is a major component of selenoproteins, including selenocysteine and selenomethionine, thus playing a key role in the activation of Se-dependent enzymes that stabilize cell metabolism [13,14]. In addition, Se modulates germ cells function and maintains reproductive integrity, through the activation of mitochondrial biogenesis [15]. The preventive role of Se in sperm and Sertoli cells (SCs) apoptosis induced by the environmental toxicant di(2-ethylhexyl) phthalate (DEHP) was also reported [16]. Thus, it may have the potential to counteract the deleterious effects of DOX on male reproductive cells.

Cyclic thioamides (e.g. propyltiouracil, carbimazole and methimazole) are antioxidant drugs used to treat thyrotoxicosis [17]. Some of these drugs were reported to inhibit sexual steroid production as side-effect, with a concurrent lower sperm quality and leading to infertility in the most severe cases [18,19]. However, the reports concerning the effects of thioamides-based therapy in male infertility are scarce. Recently, we have synthetized a new derivative of thioamide, thiocyanoacetamide (TA), which has a potent antioxidant potential [20] and ability to reduce DOX-induced toxicity in rat testis [21].

Within the testicular environment, SCs are responsible for the physical and nutritional support of spermatogenesis [22]. SCs are essential for gonadal homeostasis through their complex interactions with germ cells, Leydig and myoid cells [23,24]. Impairment of SCs function by toxicants may compromise spermatogenesis and hence male fertility [25]. Therefore, *in vitro* SCs are an adequate model to study toxicant-mediated injury in testis [26]. Previous studies reported that DOX can alter the structure and function of SCs *in vivo* [4,27]. However, the underlying mechanisms are not known. The objective of this study was to evaluate the possible protective role of TA or Se against DOX-induced *in vitro* toxicity in rat SCs, in comparison to Se.

2. Materials and methods

2.1. Chemicals

DOX was complimentary provided by Salah Azaiez Institute of Oncology (Tunis, Tunisia), under the commercial name Adriamycin® (0.9% NaCl). Se (sodium selenite pentahydrate; Na_2O_3Se) was dissolved at 50 μg/ml in pure water and purchased from Oligosol® (Paris, France). TA was produced in crystalized form in the Laboratory of Organic Synthesis and Heterocyclic of the Faculty of Sciences (Tunis, Tunisia) as previously described [21]. RMPI-1640 with L-glutamine (R6504-1L), Anti-dinitrophenyl (DNP) Rabbit monoclonal antibody (mAB) (#D9656-2 ML) and Caspase-3 Assay kit Colorimetric (CASP-3-C) were obtained from Sigma-Aldrich (St-Louis, MO, USA). LDH cytotoxicity assay kit (#88953) and BCA protein assay kit (#23225) were purchased from Thermo Fisher Scientific (Waltham, MA, USA). MTT (#0793-1G) was obtained from Amresco (Solon, OH, USA). Hoechst 33324 (H3570) was purchased from Life Technologies (Camarillo, *CA*, USA). Anti-3-nitrotyrosine (Anti-3-NT) (ab61392) and anti-4-Hydroxynonenal (Anti-4-HNE) (ab48506) antibodies were obtained from Abcam (Cambridge, UK). Anti-Bax (#2772) and anti-Bcl2 (#2870) antibodies were purchased from Cell Signaling Technology (Danvers, MA, USA).

2.2. Thiocyanoacetamide (TA) synthesis

The synthesis of the 2-cyano-2-p-nitrophenyl-Nbenzylthioamide or TA was performed as described in Fig. 1A. TA was produced in a nitrogen atmosphere; 5.6 g *per* % of potassium tert-butylate (terBuOK) dissolved in tetrahydrofuran (THF) that was previously mixed with 11.7 g *per* % of *p*-nitrobenzyl-cyanide. The mixture was stirred for 40 min, then 11.8 g *per* % of benzyl-isothiocyanat in dissolved TFH were added. The mixture was further stirred for 3 h and hydrolyzed with HCl (12 N). Extraction was then performed by adding 30 ml chloroform to the mixture and allowing it to dry. To purify the extract, ether recrystallization was processed. Purity was assessed by the extract melting point (124 °C), and by High Performance Liquid Chromatography (HPLC) using an RP18 column and UV detector set at 250 nm. Mobile phase (water/acetonitril) was pumped at a flow rate of 2 ml/min in a gradient mode as follows: 100% ultra-pure water for 0.01 min, 75% for 3.1 min, 66% for 9.1 min, 0% for 20 min and 100% for 22 min.

2.3. Cell culture and experimental design

Rat SCs (SerW3) were cultured in Cell + culture flasks (Sarstedt, Nümbrecht, Germany) and incubated at 37 °C in a humidified atmosphere with 5% CO_2. Cells were maintained in culture medium composed of RPMI-1640 supplemented with $NaCO_3$ (23.8 mM), HEPES (14.9 mM), D-glucose (14.1 mM), Fetal Bovine Serum (FBS) (10% v/v) and 1% antibiotics, including gentamycin (0.002 U/ml), penicillin (100 U/ml) and streptomycin (100 U/ml). Cells were plated and harvested for different drug tests into 96-well sterile microplates. After reaching a 70-80% of cellular confluence, the medium was replaced by RPMI medium without FBS, but supplemented with Insulin (10 mg/L) and Transferrin (5.5 mg/L) (IT). Moreover, this medium was supplemented with different

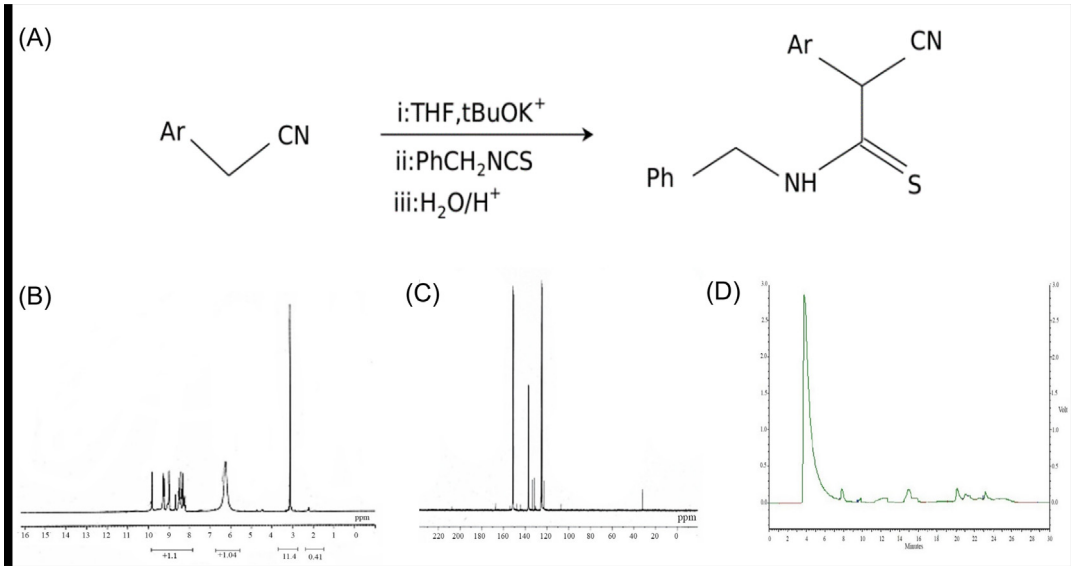

Fig. 1. (A) Chemical synthesis of the new thiocyanoacetamide (TA). In the presence of strong base, such as potassium ter-butylate (tBuOK) dissolved in tetrahydrofuran (THF) and p-nitrobenzyl-cyanide, arylacetonitriles reacts with benzyl-isothiocyanat (NCS) and lead to the formation of the 2-cyano-2-p-nitrophenyl-Nbenzylthioamide. (B–C) Graphics of ^{1}H and ^{13}C NMR spectra (400 MHz) performed for the structural identification of TA. (D) Chromatograph obtained by High Performance Liquid Chromatography (HPLC), showing a unique peak at 4.5 min of retention time corresponding to TA.

concentrations of Se, TA and DOX to create 14 different experimental conditions: Control (CTR; RPMI + IT medium), 1 μM DOX, 12 μM Se, 25 μM Se, 50 μM Se, 0.25 mM TA, 0.5 mM TA, and 1 mM TA alone or in combination with 1 μM DOX. The selection of DOX dose was based on previous studies [28,29]. TA and Se doses were selected and adjusted according to a pilot cytotoxicity analysis based on a dose-response effect when combined with DOX (data not shown). After cytotoxicity screening by MTT, LDH release and $\Delta\Psi_m$ measurement, 25 μM Se and 0.25 mM TA were selected for the further experiments. As DOX treatment generally results in cell death in a time-dependent way (8–16 h) with a maximal caspase-3 activity after 24 h [30], the incubation period for all the experimental conditions was set to 24 h.

2.4. MTT assay

MTT assay is based on the ability of mitochondrial oxidoreductase enzymes, in functional viable cells, to reduce the yellow 3-(4,5-dimethylthiazol-2-yl)-2,5-diphenyl-2H-tetrazolium bromide (MTT) to its purple insoluble formazan. Thus, this colorimetric assay measures cell metabolic activity, and represents an accurate indirect measure of cell viability. SCs were seeded into a 96-well microplate. After reaching a 90-95% confluence, cells were exposed to the different drug-supplemented media for 24 h. Then, cells were washed twice with PBS, and culture medium was replaced by 150 μl of freshly prepared IT and 15 μl of the MTT stock solution (5 mg/ml in PBS). Cells were incubated at 37 °C for 3 h and protected from the light. Subsequently, media was removed and 100 μl of dimethylsulfoxide (DMSO) were added to dissolve formazan crystals. Absorbance was measured at 570 nm to quantify formazan formation and at 655 nm for internal reference, using an iMark™ Microplate Absorbance Reader, Bio-Rad (Warszawa, Poland). Non-specific substrate reduction was normalized to the blank. Results were expressed in fold variation to CTR group.

2.5. Propidium iodide (PI) staining

PI staining was performed in the selected doses only to provide further confirmation of MTT results and to observe cell death. PI is a popular red-fluorescent agent that is not permeant to live cells, thus being useful to differentiate necrotic, apoptotic and healthy cells based on membrane integrity. SCs were seeded on coverslips into 12-well plates. When 100% confluent, cells were incubated for 24 h with the drug-supplemented media: Control (RPMI + IT medium), 1 μM DOX, 25 μM Se, 0.25 mM TA, 1 μM DOX + 25 μM Se and 1 μM DOX + 0.25 mM TA. At the end of the incubation, cells were washed twice with PBS, and fixed for 10 min in 4% paraformaldehyde in PBS. Cells were stained with 1 μg/ml PI for 10 min at RT, then mounted on slides and examined under a Nikon fluorescence microscope (Tokyo, Japan). PI yield a red fluorescence in dead cells due to membrane integrity loss. DOX autofluorescence was considered and the signal was deducted from the images. Processing was made using NIS-Elements Research Software.

2.6. LDH assay

The colorimetric LDH assay kit was used to determine cytotoxicity in SCs subjected to the experimental conditions by assessing LDH activity in the extracellular media. LDH is a cytosolic enzyme that can be released into the culture medium upon cell death due to damages in the cellular plasma membrane. Thus, the increase in LDH extracellular activity reflects an increase in the number of lysed cells. Briefly, after 24 h of exposure to the drug-supplemented media, extracellular media were transferred into a 96-well clear bottom microplate (50 μl/well). Then, 50 μl of LDH substrate were added to each well and incubated at room temperature (RT) for 30 min. To stop the reaction, a stop solution (50 μl) was added to each well. Absorbance was measured at 490 and 630 nm by Synergy™ HTX Multi-Mode Microplate Reader, BioTek (Winooski, VT, USA). Results were normalized to the blank and results are expressed in fold variation to CTR group. LDH enzymatic activity was calculated as units *per* milligram of protein using the molar extinction factor (ε) and finally expressed as fold variation to the control group.

2.7. Mitochondrial membrane potential ($\Delta\Psi_m$) assay

Mitochondrial membrane potential (ΔΨm) was determined by fluorescence microscopy using JC-1 dye after 24 h exposure to the experimental media. The accumulation of JC-1 in mitochondria depends on the ΔΨm of the cells. Red fluorescence reflects cells with functional mitochondria (JC-1 aggregates), while green fluorescence reflects cells with dysfunctional mitochondria (JC-1 monomers). A decrease in the red/green fluorescence intensity ratio indicates mitochondrial depolarization. Briefly, cells were seeded in a 96-well microplate and also on sterile coverslips into a glass-bottom plate. Cells with 80% confluence were treated with the different media for 24 h. Cells treated with FCCP (50 μM) were considered as positive control. SCs seeded on coverslips were only treated with the selected media. At the end of treatment, cells were washed twice with PBS and 50 μl of JC-1 (1 μg/ml) were added. Cells were incubated for 30 min at 37 °C and then washed 2 times with PBS. SCs in 96-well microplate were resuspended in IT medium, and fluorescence was determined at 530/590 nm using a Synergy™ HTX Multi-Mode Microplate Reader, BioTek (Winooski, VT, USA). The aggregates/monomers ratio was calculated for each condition as a measure of ΔΨm. Furthermore, SCs on coverslips were mounted on slides to be observed under a Nikon fluorescence microscope (Tokyo, Japan). DOX autofluorescence was considered and the signal was deducted from the images. Processing was made using NIS-Elements Research Software.

2.8. Protein extraction and quantification

SCs were seeded into ⌀60 mm culture dishes. Six dishes were considered *per* experimental condition (N = 6). Dishes were kept at 37 °C and 5% CO_2 until reaching 80% confluence and then treated for 24 h with the selected media. SCs were detached from the dishes with trypsin and isolated by centrifugation for total protein extraction. Total proteins were extracted using M-PER Mammalian Protein Extraction Reagent according to manufacturer's instructions. Protein quantification was made using the BCA kit as described by the manufacturers.

2.9. Slot-blot assay

Protein oxidation and lipid peroxidation are often used as biomarkers for oxidative stress and they can be evaluated by measuring their resulting products such as 2,4-dinitrophenyl (DNP), nitro-tyrosine and 4-hydroxynonenal (4-HNE). The content of these adducts were measured in SCs after exposure to the different experimental groups, to evaluate carbonyl groups, protein nitration and lipid peroxidation, respectively, using the Slot Blot assay as previously described [31]. Membranes were incubated overnight (4 °C) with primary antibodies: rabbit anti-DNP, rabbit anti-nitro-tyrosine or goat anti-4-HNE at 1:5000 dilutions. Then, membranes were incubated with goat anti-rabbit IgG-AP (1:5000) or rabbit anti-goat IgG-AP (1:5000) for 1 h at room temperature. Membranes were reacted with ECL substrate (GE, Healthcare, Buckinghamshire, UK) and images were acquired by ChemiDoc™ MP image analyzer, BioRad (Warszawa, Poland). Results were expressed as fold variation to CTR group.

2.10. Hoechst 33342 staining

Cells were seeded on coverslips into a glass-bottom plate and left to growth until reaching 80–90% confluence. SCs were then incubated with the different drug-supplemented media. At the end of 24 h treatment, cells were washed twice with PBS and fixed for 10 min in 4% paraformaldehyde in PBS. For morphology assessment, nuclei were stained by incubating cells with 10 μg/ml Hoechst 33342 for 10 min at RT. Coverslips were mounted onto slides and examined under a Nikon fluorescence microscope (Tokyo, Japan). Nuclear alterations were identified according to chromatin condensation, fragmentation and bright staining. Nuclei uniformly stained blue were considered normal. In each group, 10 random visual fields and >300 cells *per* field were counted. Apoptotic cell percentages were averaged out of six different fields for each condition and results were expressed in fold variation to CTR group.

2.11. Western blot

Western blot analysis was carried out as previously reported [31]. 30 μg of protein were used. Bax and Bcl-2 protein expression was detected using specific antibodies, and β-actin was used as protein loading control for relative quantification. Membranes were reacted with ECL substrate (GE, Healthcare, Buckinghamshire, UK) and images were acquired by ChemiDoc™ MP image analyzer, BioRad (Hercules, California, USA). Quantification of bands density was performed using Image Lab software, BioRad (Hercules, California, USA). Band densities were divided by the corresponding β-actin band density and results were expressed as fold variation to CTR group. Bax/Bcl-2 ratio was calculated afterwards.

2.12. Caspase-3 activity assay

Caspase-3 colorimetric assay was performed as described by the manufacturer's protocol (Sigma-Aldrich, St-Louis, MO, USA). Briefly, 5 μg of protein were mixed with 90 μl of assay buffer and Ac-DEVD-pNA substrate, and incubated for 120 min. The absorbance was measured at 405 nm and caspase-3 activity was calculated according to the p-nitroaniline (pNA) amount in the sample. Six independent conditions were considered *per* group. Caspase-3 activity was expressed as pmol of pNA/μg of protein/min.

2.13. Autophagy assay

Cells were grown in a 96-well microplate until reach 89-90% confluence. After 24 h exposure to the selected drug-supplemented media, SCs were incubated with 1 μg/ml Hoechst 33342 for 10 min, in the dark, at RT. Then, cells were washed twice with PBS and stained with 1 μg/ml of monodansylcadaverine (MDC) for 10 min, at 37 °C. Cells were washed again with PBS and 100 μl of fresh PBS were added to each well. Fluorescence was immediately analyzed at the respective Hoechst and MDC excitation/emission wavelengths (360/460 nm and 360/528 nm), using a Synergy™ HTX Microplate Reader, BioTek (Winooski, VT, USA). Results were normalized to the number of cells and expressed as fold variation to the CTR group.

2.14. Statistical analysis

All numerical data are expressed as mean ± SEM (N = 6). Statistical analysis was conducted using GraphPad ® (San Diego, CA, USA). Data were checked for normality using Shapiro–Wilk test and significance was determined using Student'*t*-test. Results were considered statistically significant for $P < 0.05$.

3. Results

3.1. Characterization of the synthesized thiocyanoacetamide (TA)

The structural identification of TA by infrared radiation (IR) showed the following results: ($CHCl_3$, ν cm^{-1}): NH = 3311,

−SH = 2540, CN = 2234.

TA analysis using Gas Chromatography–Mass Spectrometry (GC-MS) (*m*/*z*) showed the following data: 194 ($C_6H_5H_2C–HN–CH=S$), 162 ($O_2NC_6H_5–CH–CN$), 116 ($C_6H_5–H_2C–HN–CH$), 91 ($C_6H_5–H_2C$) and 77 ($C_6–H_5$).

To verify the chemical functions and to highlight the complete synthesis of TA molecule, ^1H and ^{13}C spectrum nuclear magnetic resonance (NMR) (400 MHz) were evaluated. NMR analysis showed the following results:

^1H NMR in $CDCl_3$ δ ppm 2.2 (-SH), 3.1(-CH_2), 8.8–9.4 (2 aromatic cycles: phenyls) and 9.9(−NH). ^1H NMR ($CDCl_3$, δ ppm): 3.1 (−CH_2), 8.8–9.9 (H_{arom}) and 6.3 (−NH).

^{13}C NMR in $CDCl_3$ δ ppm 32 ($O_2N–C_6H_6O–CN$), 108 (CN) and 123–155 (2 aromatic cycles: phenyls) (Fig. 1B), ^{13}C NMR δ ppm 32 ($O_2N–C_6H_6O–CN$), 108 (CN) and 123–155 (2 aromatic cycles: phenyls) (Fig. 1C).

The purity of TA was verified by high performance liquid chromatography (HPLC) at gradient mode. The chromatogram displayed a single peak at 4.5 min of retention time, which confirm the purity of the synthesized TA (Fig. 1D).

3.2. The combined treatment with TA reduced DOX cytotoxicity to Sertoli cells

Exposure of SCs to 1 μM DOX reduced metabolic viability relative to the CTR group (Fig. 2A), while increasing LDH extracellular activity (Fig. 2B). SCs exposed to the media supplemented solely with Se showed a decrease in metabolic viability (Fig. 2A). Moreover, SCs exposed to 12 μM Se showed an increase in LDH extracellular activity (Fig. 2B), but not those exposed to higher Se doses (25 μM or 50 μM). Similarly, exposure of SCs to 0.25, 0.50 or 1 mM TA, reduced the metabolic viability of SCs relative to the CTR group (Fig. 2A). However, LDH extracellular activity was not altered by exposure to any of TA doses (Fig. 2B). The combined treatment of SCs with 1 μM DOX + 12 μM Se, as well as with any of the three concentrations of TA, restored cell metabolic viability to control values (Fig. 2A). In addition, DOX (1 μM) association with 1 mM TA increased SCs metabolic activity relative to DOX-only treated cells (Fig. 2A). LDH extracellular activity was higher in all DOX + Se groups and the DOX + 0.5 mM TA group relative to the CTR. Interestingly, SCs exposed to 1 μM DOX combined either with 0.25 mM TA or 1 mM TA, showed normal LDH extracellular activity (Fig. 2B). There was also an increase in PI staining in SCs exposed to 1 μM DOX, as well as an increase in altered cell morphology along with a lower colony forming ability (Fig. 2C). Exposure of SCs to 25 μM Se or 0.25 mM TA induced an increase in PI-stained nuclei and an alteration of cell morphology relative to the CTR group. PI staining was slightly lower when DOX was associated with 25 μM Se, and further lower when DOX was combined with 0.25 mM TA. The combined treatment of DOX with TA restored the normal colonies aspect and increased cell density and agglomeration (Fig. 2D).

3.3. Combined exposure of SCs to DOX and TA did not alter mitochondrial membrane potential or oxidative stress markers

SCs exposed to the media supplemented with 1 μM DOX, 12 μM Se, 25 μM Se, 50 μM Se, 0.25 mM TA or 0.50 mM TA did not show alterations in $\Delta\Psi_m$ when compared with the CTR group (Fig. 3A). However, the supplementation with 1 mM TA induced a decrease in $\Delta\Psi_m$, whereas exposure to 1 μM DOX + 12 μM or 50 μM Se resulted in an increased $\Delta\Psi_m$ when compared to the CTR group. The exposure of SCs to the DOX + TA combinations did not result in any significant change in $\Delta\Psi_m$. These findings were further confirmed by the red/green fluorescence balance observed by JC-1 staining performed only at Se (25 μM) and TA (0.25 mM) selected doses in the test groups, which showed no significant difference in $\Delta\Psi_m$, in comparison with CTR group (Fig. 3B).

Mitochondria are the main producers of reactive oxygen species (ROS) in cells, so they reflect the cellular oxidative status. One of the main toxic effects exerted by DOX is ROS overproduction due to mitochondrial dysfunction. However, exposure of SCs to 1 μM DOX or any of the other media did not alter carbonyl groups levels, protein nitration or lipid peroxidation relative to the CTR group (Fig. 4).

3.4. The association of DOX with Se or TA decreased apoptotic cell count

DOX treatment has been associated with increased cellular apoptosis [32]. Indeed, observation of nuclei morphology by Hoechst staining revealed that 1 μM DOX induced chromatin fragmentation and condensation (Fig. 5A). This was reflected by the increase in apoptotic cell count relative to CTR group (Fig. 5B). As showed in Fig. 5A and B, cells treated with 25 μM Se or 0.25 mM TA showed no significant alterations on chromatin aspect or on apoptotic cell count. Furthermore, SCs exposure to 1 μM DOX + 25 μM Se or 1 μM DOX + 0.25 mM TA maintained nuclei morphology (Fig. 5A) and apoptotic cell count (Fig. 5B).

3.5. The combined exposure to DOX with Se or TA prevented alterations in caspase-3 activity

The intrinsic apoptosis signaling pathway is mainly controlled by the Bcl-2-family, which interacts with the major pro-apoptotic protein Bax [33], leading to the activation of caspase-3 cascade [34]. Bax and Bcl-2 protein expression, as well as the Bax/Bcl-2 ratio were similar among all the experimental groups (Fig. 6A, 6B, 6C). However, caspase-3 activity (Fig. 6D) was increased in SCs exposed to 1 μM DOX relative to the CTR group. Combined exposure of 1 μM DOX either with 25 μM Se or 0.25 mM TA was able to restore caspase-3 activity to CTR values (Fig. 6D).

3.6. The combined exposure to DOX with TA reduced autophagy in SCs

Autophagy can promote or suppress cell death and can also preserve cell integrity and metabolism in the presence of a cytotoxic agent or in pathological conditions [35]. As illustrated in Fig. 7, the exposure of SCs to 1 μM DOX had no significant effect on autophagy. The same results were observed in the group of SCs treated with 25 μM Se, 0.25 mM TA, or 1 μM DOX + 25 μM Se. However, autophagy levels were reduced after exposure to 1 μM DOX + 0.25 mM TA.

4. Discussion

Cancer is the second major cause of death. It carries the highest social and economic encumbrance due to the high costs of diagnosis, treatment and side effects [36]. During the last years, one out of 49 individuals was diagnosed with a malignant tumor during the first decades of age [37], and one out of 530 adults (20-35 years) had an infantile cancer [38]. Hence, 50% of patients diagnosed with malignant diseases were or will be prescribed a cancer therapy. Consequently, there is an increasing concern regarding the effects of these therapies on male fertility and it is recommended for many patients to undergo gamete cryopreservation [39]. However, prepubescent patients and those already suffering from poor fertility parameters are usually not eligible. Therefore, vectorized chemotherapy drugs like DOX [40] or association with natural and synthesized compounds have been tested to reduce treatment side

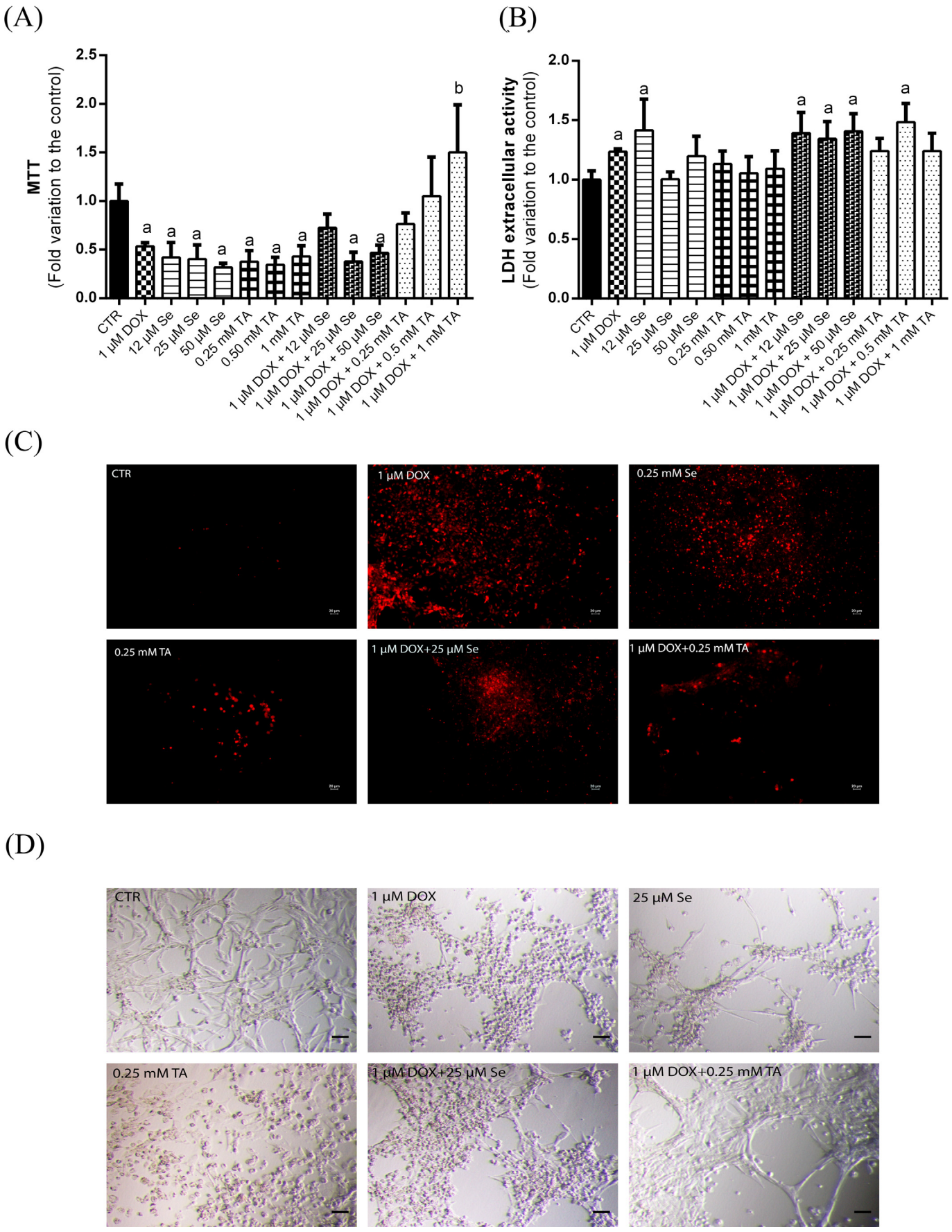

Fig. 2. Illustration of dose-dependent toxicity in Sertoli cells (SCs) exposed to culture medium supplemented with DOX (1 µM), selenium (Se - 12, 25 or 50 µM), or thiocyanoacetamide (TA - 0.25, 0.5 or 1 mM) in comparison to control (CTR) group. DOX (1 µM) was also combined with Se or TA at the same concentrations. (A) represents cells viability using MTT assay and (B) extracellular LDH activity. Each bar represents the mean ± SEM out of six replicates. Significantly different results ($P < 0.05$) are indicated as: a – relative to CTR; b – relative to DOX-only treated group. (C) represents propidium iodide (PI) staining observed under red light fluorescence microscope (scale bar = 20 µm), and (D) SCs colonies aspect observed under light microscope (400 ×) (scale bar = 50 µm).

(A)

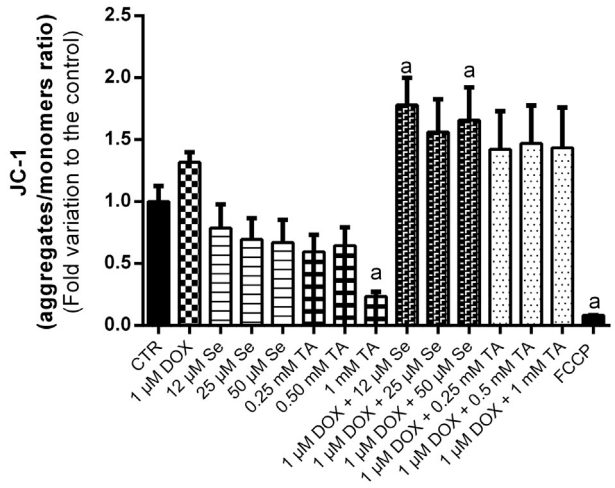

(B)

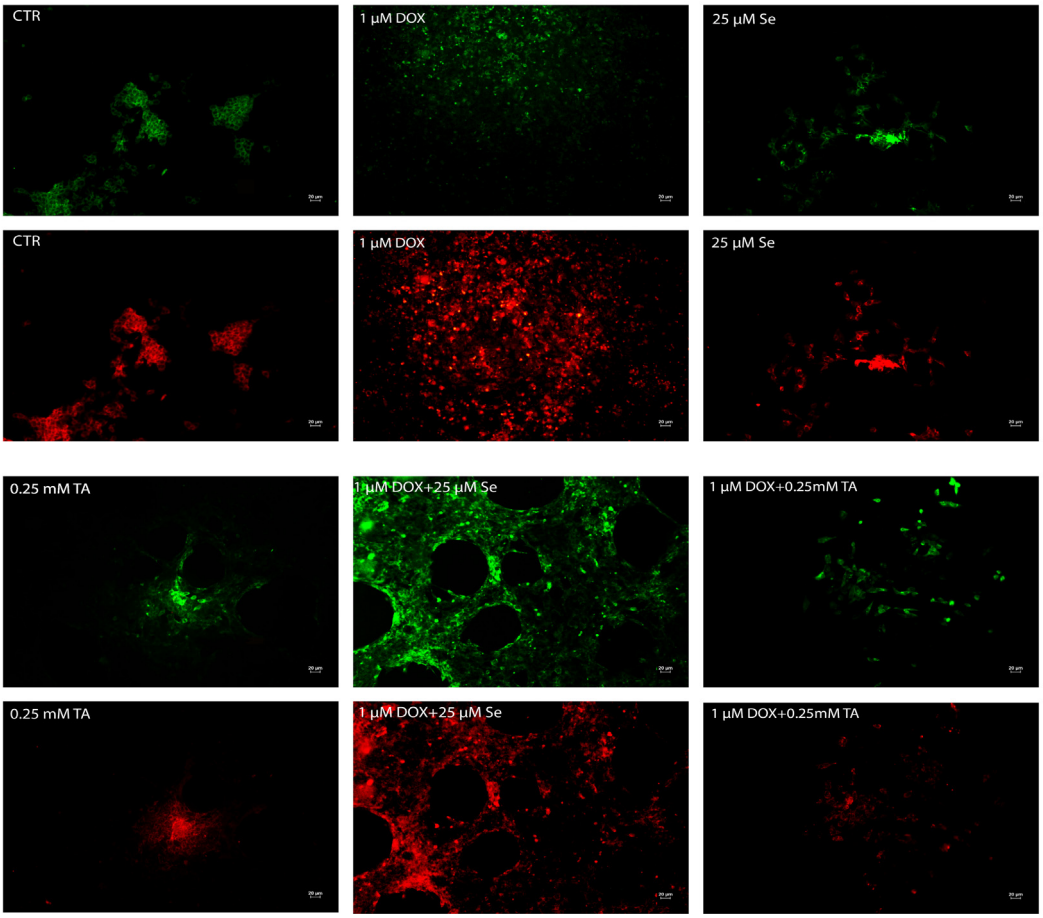

Fig. 3. Mitochondrial membrane potential ($\Delta\Psi m$) of Sertoli cells (SCs) after exposure to culture medium supplemented with DOX (1 µM), selenium (Se - 12, 25 or 50 µM), or thiocyanoacetamide (TA - 0.25, 0.5 or 1 mM) in comparison to control (CTR) group. DOX (1 µM) was also combined with Se or TA at the same concentrations. (A) Graphic representation of the averaged aggregates/monomers ratio after JC-1 fluorescent staining. Each bar represents the mean ± SEM out of six replicates. Significantly different results ($P < 0.05$) are indicated as: a – relative to CTR. (B) Representative images of green/red fluorescence intensity emitted by SCs stained with JC-1.

effects, especially its toxicity to highly proliferating cells [41].

Chemotherapeutic agents are known to disrupt spermatogenesis by affecting various testicular cells, such as Leydig cells, SCs, and germ cells [42]. Experimental evidence suggests that severe spermatogenesis impairment caused by DOX treatment is related to germ cell apoptosis and structural damage of SCs [43]. SCs play a key role in germ cell development and survival through a complex molecular interaction with the different cells within the

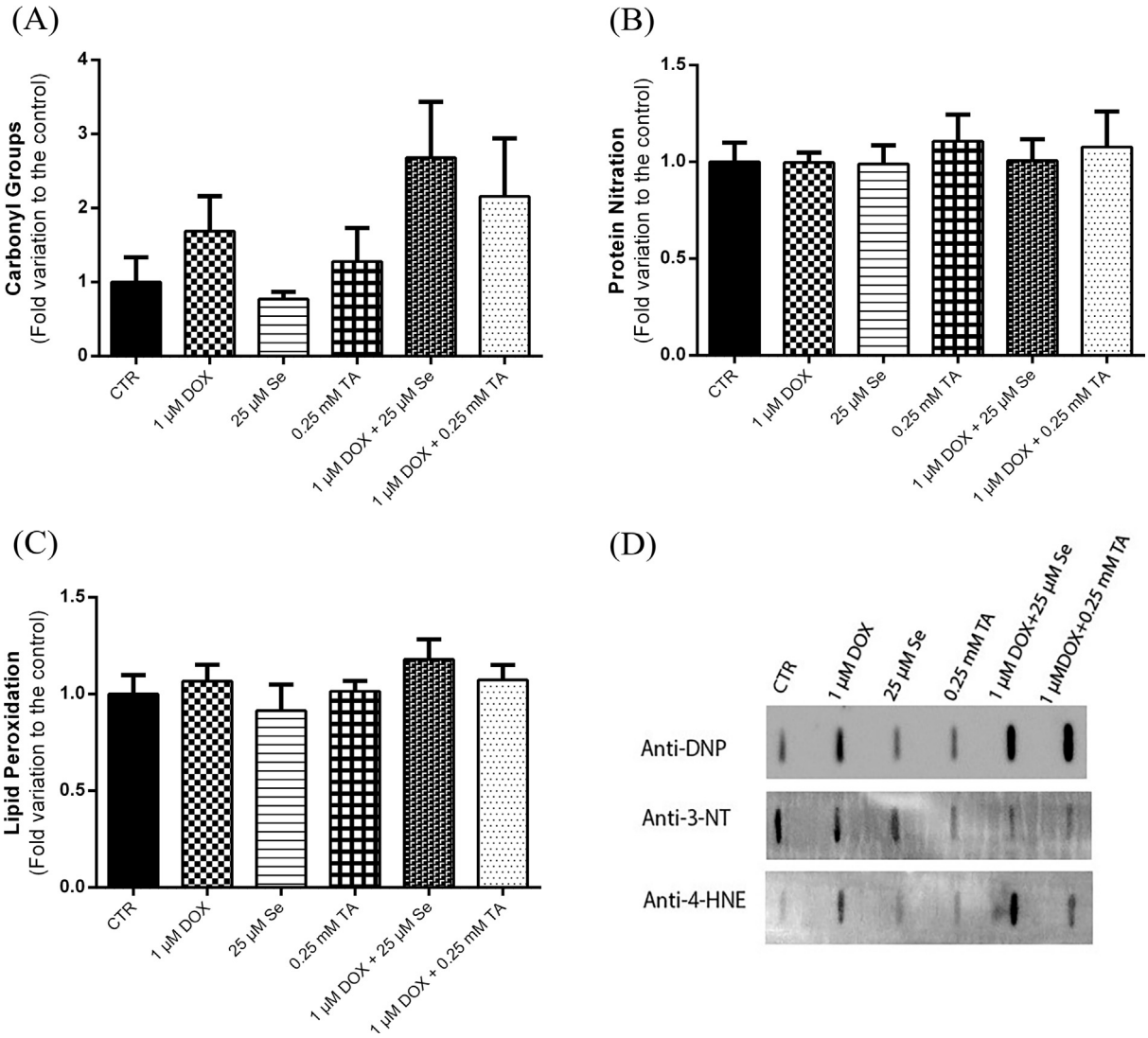

Fig. 4. Oxidative stress biomarkers after exposure of Sertoli cells (SCs) to culture medium supplemented with 1 μM DOX, 25 μM selenium (Se), or 0.25 mM thiocyanoacetamide (TA) in comparison to control (CTR) group. DOX (1 μM) was also combined with 25 μM Se or 0.25 mM TA. (A) represents carbonyl groups, (B) protein nitration, and (C) lipid peroxidation. Each bar represents mean ± SEM averaged out of six replicates. (D) displays the representative slot-blot figures (of one sample) for anti-DNP, anti-3-NT, and anti-4-HNE.

seminiferous epithelium [44]. It has been suggested that DOX-induced damage to SCs results in germ cell injury in animal models [4,45]. Still, the mechanisms by which DOX induces SCs toxicity are not known. Our work was designed to study the direct effects of DOX in rat cultured SCs, and to evaluate the protective potential of Se and TA against DOX cytotoxicity.

Reduced cell viability and increased LDH release after SCs treatment with 1 μM DOX were regarded as the first signs of DOX-induced toxicity. Sadeghi-Aliabadi et al. [29] and Tomankova et al. [46] also described a significant decrease in Hela and MCF7/NIH3T3 cells viability after exposure to 1 μM and 0.5 μM DOX, respectively. Holmgren et al. [47] reported a progressive increase in LDH level in the extracellular medium after cardiomyocytes exposure to 0.4 μM DOX. Media supplemented with Se (12, 25 or 50 μM) or TA (0.25, 0.50 or 1 mM) presented some cytotoxicity to SCs as reflected by the decrease in cell metabolic viability by MTT assay. Although Se toxicity was not more severe than that of DOX, Se association with DOX seemed to be more lethal to SCs. Recently, another study with bovine SCs also reported a cytotoxic effect of certain Se doses [48]. Despite, based on MTT results DOX association with the three concentrations of TA sustained cell survival, suggesting a potent TA ability to counteract DOX-mediated death. Moreover, DOX association with 0.25 mM or 1 mM TA prevented an increase of LDH release and only 1 μM DOX + 0.50 mM TA significantly promoted extracellular LDH release. LDH is a cytosol enzyme that only crosses the plasmatic membrane when this structure is compromised. Extracellular LDH activity is correlated to cytotoxicity and is frequently used as a marker of cell death by necrosis [49]. Thus, we suggest that DOX may lead to SCs death by necrosis and TA supplementation showed higher efficacy in reducing DOX-triggered cytolysis.

Mitochondria are essential for cell function as they are the main energy source [50]. Some uncoupling agents such as DOX target mitochondria by altering mitochondrial membrane stability, which is a crucial event that determines cell subsistence or death [51]. Previous studies reported that DOX toxicity can lead to mitochondrial dysfunction [52]. Despite the previous observations suggesting that DOX causes $\Delta\Psi_m$ loss in human carcinoma cells, we did not observe any changes in SCs exposed to 1 μM DOX [53]. Besides, some studies reported that Se does not affect mitochondrial function and biogenesis in healthy cells [54,55], whereas others showed a Se-induced prevention of mitochondrial potential collapse in cells

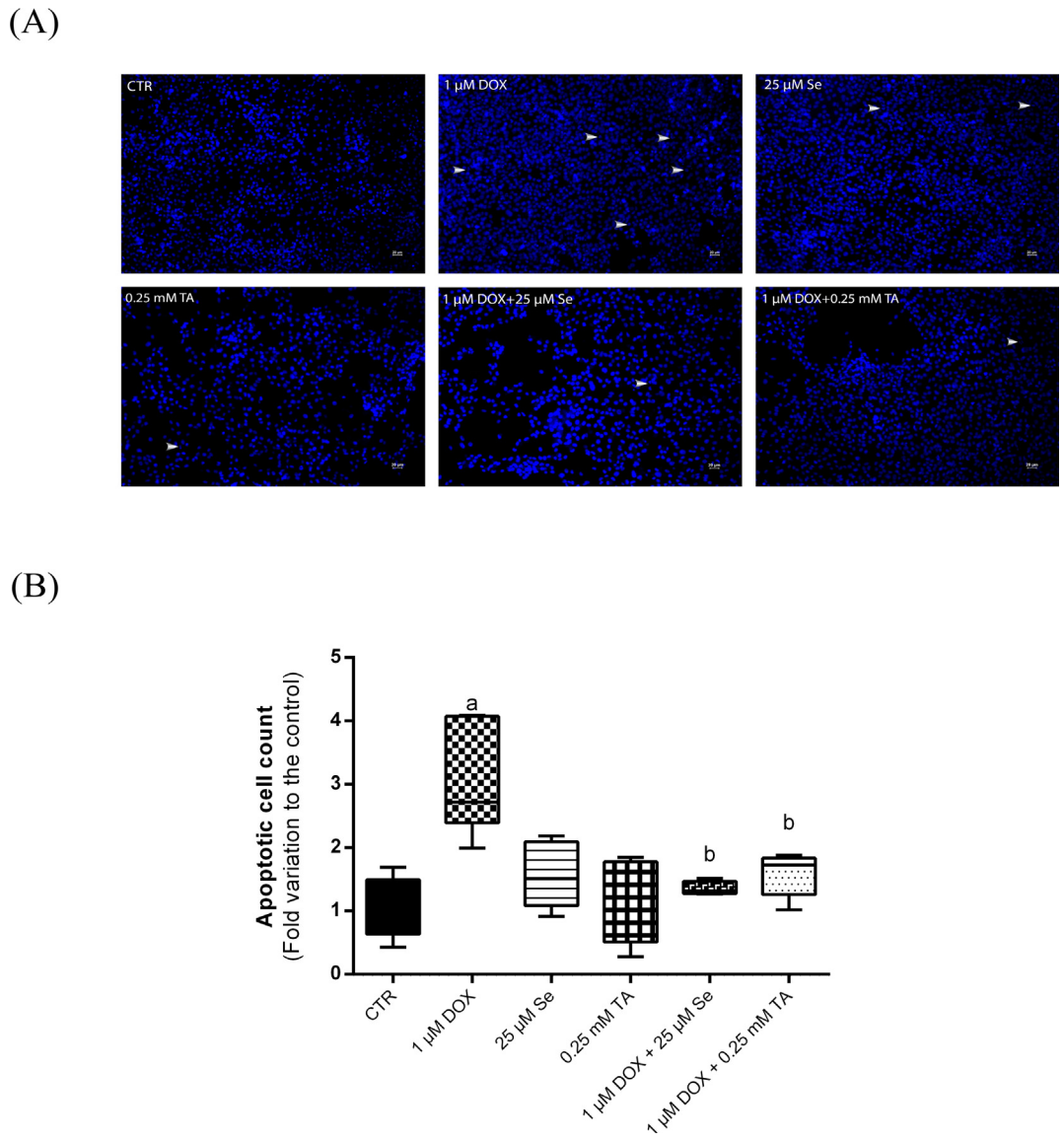

Fig. 5. Figure (A) shows representative images of chromatin aspect of Sertoli cells (SCs) after exposure to culture medium supplemented with 1 µM DOX, 25 µM selenium (Se), or 0.25 mM thiocyanoacetamide (TA) in comparison to control (CTR) group. DOX (1 µM) was also combined with 25 µM Se or 0.25 mM TA. Morphological changes in nuclei (chromatin fragmentation and condensation) were observed using a blue filter in a fluorescence microscope and are represented by an arrow head. Figure (B) provides a graphic illustration of apoptotic cells count in the different groups. Each bar represents mean ± SEM averaged out of six different fields for each condition. Significantly different results ($P < 0.05$) are indicated as: a – relative to CTR; b – relative to DOX-only treated group.

subjected to cytotoxic stress [56,57]. In our study, none of the tested doses of Se affected $\Delta\Psi_m$ when administered alone. Additionally, TA administration at 0.25 mM and 0.50 mM had no significant effect on $\Delta\Psi_m$, but the 1 mM TA formulation induced a reduction in $\Delta\Psi_m$ of SCs. The administration of 12 µM or 50 µM Se in combination with DOX, resulted in a higher $\Delta\Psi_m$. However, DOX association with 25 µM Se did not affect $\Delta\Psi_m$, which mainly contributed to the selection of this Se dose for further evaluation. An increased $\Delta\Psi_m$ is usually associated with an enhancement of ATP production, but it can also lead to oxidative imbalance [58]. In fact, a 10% variation in $\Delta\Psi_m$ in healthy cells may result in a 90% drop in ATP synthesis and 90% increase in ROS generation [59]. In this regard, we suggest that DOX association with the lowest and the highest dose of Se is noxiously affecting mitochondrial function, though, DOX association with the three doses of TA had no significant effect on $\Delta\Psi_m$ (Fig. 4A and B). As 0.50 mM TA promoted LDH extracellular activity and 1 mM TA collapsed $\Delta\Psi_m$, 0.25 mM TA was the selected dose for further studies.

The maintenance of homeostasis between ROS and ATP production by mitochondria is pivotal as it usually reflects the energy requirements in specific physiological condition [60]. Besides $\Delta\Psi_m$, ROS measurement provides essential clues about cell functioning. Thus, we measured some oxidative stress and apoptosis markers in SCs. DOX is considered as an exogenous inducer of ROS production in mitochondria [61]. Contrary to Zhao et al. [62] who showed that DOX induces mitochondrial dysfunction and lipid peroxidation in mouse heart mitochondria and Wei et al. [63] who reported an overproduction of ROS in mouse embryonic fibroblasts, we found that supplementation of 1 µM DOX in culture medium did not promote oxidative damage (protein nitration/carbonylation or lipid peroxidation) in SCs. This may be due to the different sensitivity to chemotherapy drugs between cell types. Few studies have described molecular events responsible for oxidative stress in SCs. Unlike germ cells, which are highly sensitive to oxidative damage,

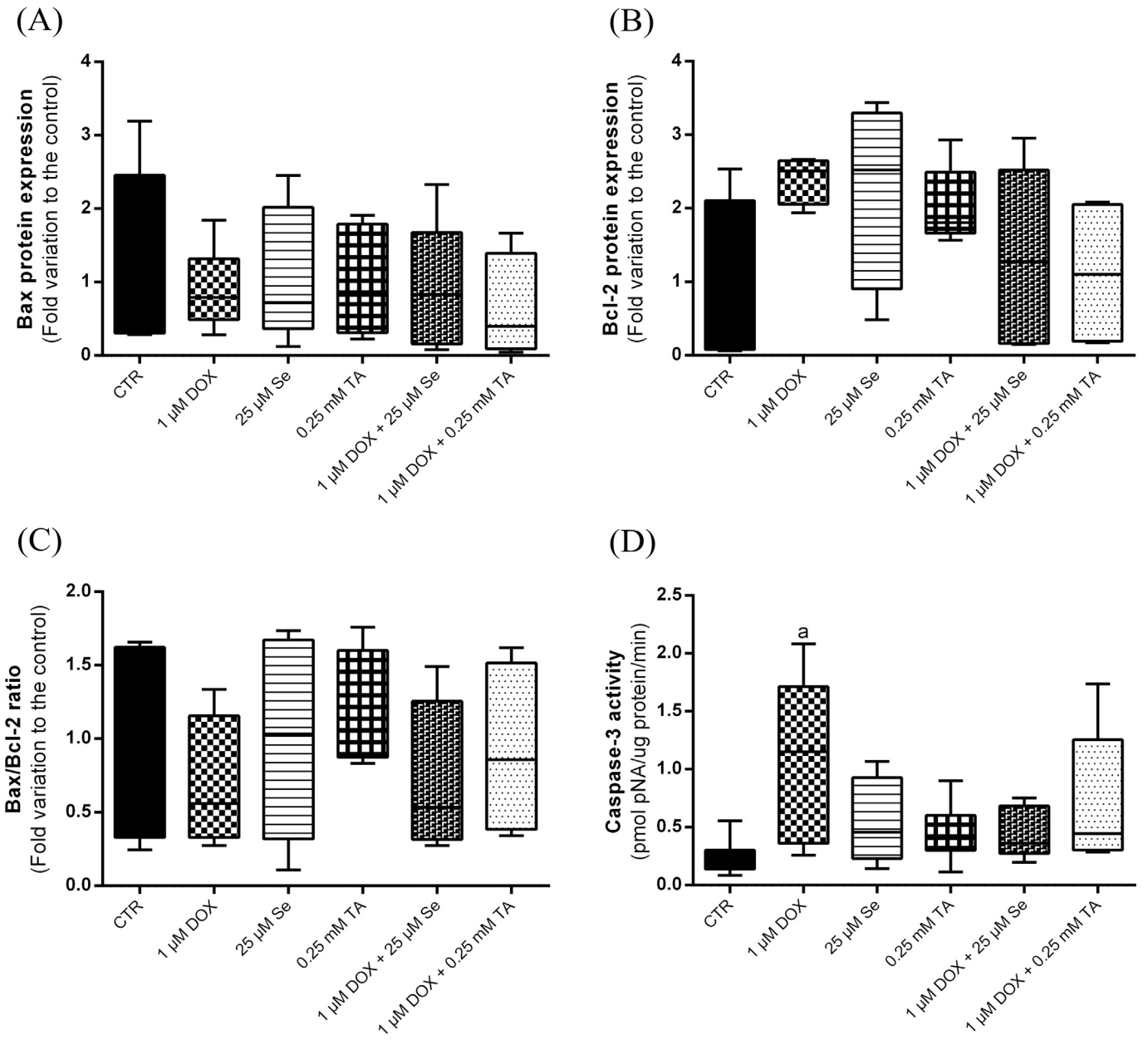

Fig. 6. Graphic illustration of (A) Bax protein expression, (B) Bcl-2 protein expression, (C) Bax/Bcl-2 ratio and (D) caspase-3 activity in Sertoli cells (SCs) after exposure to culture medium supplemented with 1 μM DOX, 25 μM selenium (Se), or 0.25 mM thiocyanoacetamide (TA) in comparison to control (CTR) group. DOX (1 μM) was also combined with 25 μM Se or 0.25 mM TA. Each bar represents mean ± SEM averaged out of six independent experiments. Significantly different results ($P < 0.05$) are indicated as: a – relative to CTR.

SCs minimize ROS and free radical reactivity by modulating their intracellular antioxidant defenses [64].

Differential DOX-induced cell death processes have been extensively described, including necrosis [9], mitotic catastrophe [65], apoptosis [66] and autophagy [67]. $\Delta\Psi_m$ disturbance has been frequently considered as the point of no return in apoptosis activation, which consequently stimulates caspase activity and cell death [68]. $\Delta\Psi_m$ loss and ROS generation are not the only triggers for apoptosis [69]. The potent antitumor activity of DOX is related to its ability to intercalate DNA, thus fostering DNA damage, which is a stimuli for apoptosis [70]. DOX-induced apoptosis involves the activation of signaling cascades through caspase-3 [32]. DOX was reported to activate diverse regulatory factors, such as CENP-A, Mad2, BubR1, and Chk1, leading to apoptosis in different human hepatoma cell lines [65]. Besides, DOX increased Bax/Bcl-2 mRNA expression in MCF-7 cells [71]. Huigsloot et al. [30] reported that DOX can overexpress Bcl-2 protein in breast cancer cells, further eliciting the pro-apoptotic effect of DOX through the Bax/Bcl-2 pathway. In our observations, Bax and Bcl-2 protein expression was unchanged after exposure to DOX, but there was a significant increase in apoptotic cells count. As caspase activation is a downstream event in apoptosis, we also quantified caspase-3 activity. Our findings revealed that DOX significantly stimulates caspase-3 activity. Caspase-3 activation is intrinsic when the signaling cascade is triggered by cytochrome *c* release and caspase-9 activity and extrinsic if the pathway is activated via membrane death receptors [72]. When caspase-3 activity reaches a threshold, it triggers alternative apoptotic pathways, such as MEK/ERK [73] or NF-κB [74]. In our work, we report that Se combination with DOX decreased SCs apoptosis, as showed by the lower number of

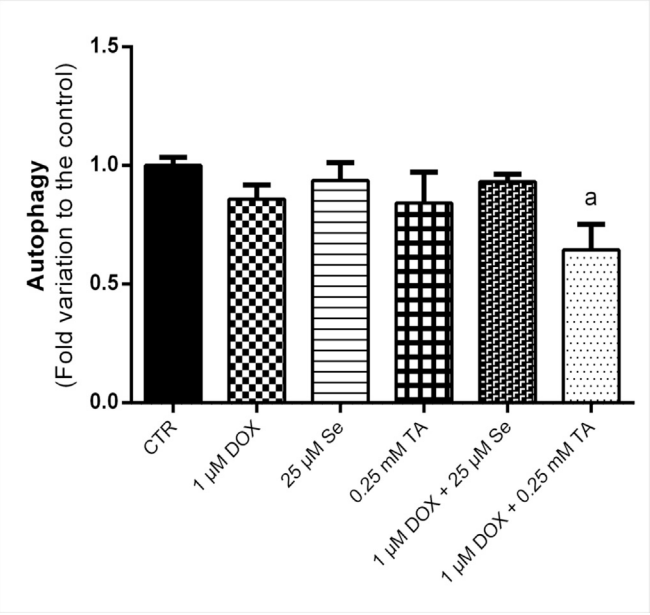

Fig. 7. Autophagy in Sertoli cells (SCs) upon exposure to culture medium supplemented with 1 μM DOX, 25 μM selenium (Se), or 0.25 mM thiocyanoacetamide (TA) in comparison to control (CTR) group. DOX (1 μM) was also combined with 25 μM Se or 0.25 mM TA. Each bar represents mean ± SEM averaged out of six different replicates. Significantly different results ($P < 0.05$) are indicated as: a – relative to CTR.

apoptotic cells (Fig. 5B) and decreased caspase-3 activity (Fig. 6B). Still, cell survival was not promoted, which suggest an alternative death process other than apoptosis in SCs exposed to these test compounds. Several studies reported a synergistic effect between DOX and Se in apoptosis, through Fas signaling activation [75] or P-53/MAPKs [76] in different cancer cell lines. Other reports suggested that Se may inhibit normal cells from entering apoptosis, such as demonstrated in prostate cells [77], human lens epithelial cells [78], or neural cells [79]. We hypothesized that Se may decrease DOX-induced apoptosis in SCs, yet it does not prevent cell death through different pathways. A similar effect was observed when TA was associated with DOX. This new molecule showed capacity to enhance SCs viability and lowered the increase in caspase-3 activity and apoptotic cells count induced by DOX treatment. Our results highlight TA capacity to diminish DOX-induced toxicity in SCs. Yet, the precise molecular mechanisms and signaling pathways need to be further investigated.

Emerging evidences appoint toward a convergence between apoptosis and autophagy and shows that DOX-affected cell functioning depends on autophagy initiation through different approaches [80,81]. A crucial concept often misjudged is that, even when autophagy modulates cell death, there is not necessarily a direct link between autophagy and cell death pathways [82]. Reports frequently described a connection between the controlling machinery that regulates autophagy and apoptosis, including PI3 kinase/Akt pathway [83] and the upregulation of *P-53* gene expression [84]. The regulation of apoptosis and autophagy is synchronized and autophagy can be a limiting or a promoting factor of apoptosis [85]. DOX has been shown to upregulate autophagy related genes (*Atg*) [86], thus contributing to DOX-induced toxicity [10,87]. We evaluated autophagy (or the self-degradation process) in SCs exposed to the different drugs. Contrary to previous studies and showing that DOX modulates autophagy in hepatocellular carcinoma cells [73] and cardiomyocytes [88], we did not observe any significant change in autophagy of SCs exposed exclusively to DOX. We suppose that there has been a major pro-apoptotic stimulation by DOX at the expense of autophagy. Our results were in accordance with those observed by Tacar et al. [89] who reported a predominance of apoptotic death in isolated human osteosarcoma and cardiomyocyte cell lines exposed to DOX. Besides the fact that autophagy and apoptosis can be coincident or antagonistic events [35], autophagic death is stimulated only when apoptosis is compromised even if DNA damage occurs [90]. The unaffected autophagy of SCs by DOX exposure might be a consequence of an early apoptosis activation. On the other hand, autophagy was decreased in SCs exposed to a combination of DOX and 0.25 mM TA. As discussed above, TA combination with DOX decreased DOX-mediated apoptotic death and improved cell viability. In this regard, we supposed that decreased autophagy is whether due to lower degradation and recycling rate of biomolecules to supply the energy needs of the cell, or TA may control DOX cytotoxicity. As the combined treatment of DOX and TA apparently decreased DOX pro-apoptotic action and promoted cell survival, we considered that autophagy drop could be a protective response of SCs against DOX toxicity. Nevertheless, autophagy and programmed cell death are still controversial and further studies are needed to clarify our hypothesis.

In summary, strategies to improve life quality of patients undergoing chemotherapy mostly rely on the physiological differences between tumor and healthy cells, but also on treatments that protect normal cells activity. Our study is the first report showing that SCs exposure to DOX leads to a lower cell viability, affects intracellular and extracellular LDH level, and stimulates apoptotic death through caspase-3 activation independently of Bax/Bcl-2 expression. Yet, DOX treatment had no effect on $\Delta\Psi_m$, autophagy and oxidative stress biomarkers. $\Delta\Psi_m$ loss, ROS production, caspase activation and Bax/Bcl-2 response are independent events in DOX-treated SCs, but it might trigger alternative cell death signaling pathways. Both combined treatments averted DOX-induced apoptosis and TA showed better efficiency to reduce DOX-induced cell death relative to Se. In the context of chemoprevention strategies, further studies must be performed to identify TA mechanisms of action, as well as the ideal doses, time of exposure and potential benefits for an optimal efficacy as co-adjuvant therapies.

Conflicts of interest

The authors declare that they have no conflicts of interest.

Acknowledgements

This work was supported by “Fundação para a Ciência e a Tecnologia” - FCT to Tânia R. Dias (SFRH/BD/109284/2015), Luís Crisóstomo (SFRH/BD/128584/2017). The work was co-funded by FEDER through the COMPETE/QREN, FSE/POPH to Marco G. Alves (PTDC/BIM-MET/4712/2014); Pedro F. Oliveira (PTDC/BBB-BQB/1368/2014); UMIB (PEst-OE/SAU/UI0215/2014); co-funded by the EU Framework Program for Research and Innovation H2020 (POCI/COMPETE2020). The authors are thankful to the Tunisian Ministry of Superior Education and Research for its financial support.

References

[1] McGuire S. World cancer report 2014, vol. 7. Geneva, Switzerland: World Health Organization, International Agency for Research on Cancer, WHO Press; 2015. p. 418–9. Adv Nutr 2016.
[2] Oeffinger KC, Mertens AC, Sklar CA, Kawashima T, Hudson MM, Meadows AT, et al. Chronic health conditions in adult survivors of childhood cancer. N Engl J Med 2006;355:1572–82.
[3] Pelicano H, Carney D, Huang P. ROS stress in cancer cells and therapeutic implications. Drug Resist Updates 2004;7:97–110.
[4] Brilhante O, Okada FK, Sasso-Cerri E, Stumpp T, Miraglia SM. Late

morfofunctional alterations of the Sertoli cell caused by doxorubicin administered to prepubertal rats. Reprod Biol Endocrinol 2012;10:79.
[5] Lipshultz SE, Miller TL, Lipsitz SR, Neuberg DS, Dahlberg SE, Colan SD, et al. Continuous versus bolus infusion of doxorubicin in children with ALL: long-term cardiac outcomes. Pediatrics 2012;130:1003–11.
[6] Hilmer SN, Cogger VC, Muller M, Le Couteur DG. The hepatic pharmacokinetics of doxorubicin and liposomal doxorubicin. Drug Metab Dispos 2004;32:794–9.
[7] Carvalho C, Santos RX, Cardoso S, Correia S, Oliveira PJ, Santos MS, et al. Doxorubicin: the good, the bad and the ugly effect. Curr Med Chem 2009;16:3267–85.
[8] Buchholz TA, Stivers DN, Stec J, Ayers M, Clark E, Bolt A, et al. Global gene expression changes during neoadjuvant chemotherapy for human breast cancer. Cancer J 2002;8:461–8.
[9] Sugimoto K, Tamayose K, Sasaki M, Hayashi K, Oshimi K. Low-dose doxorubicin-induced necrosis in Jurkat cells and its acceleration and conversion to apoptosis by antioxidants. Br J Haematol 2002;118:229–38.
[10] Wang X, Wang XL, Chen HL, Wu D, Chen JX, Wang XX, et al. Ghrelin inhibits doxorubicin cardiotoxicity by inhibiting excessive autophagy through AMPK and p38-MAPK. Biochem Pharmacol 2014;88:334–50.
[11] Minotti G, Menna P, Salvatorelli E, Cairo G, Gianni L. Anthracyclines: molecular advances and pharmacologic developments in antitumor activity and cardiotoxicity. Pharmacol Rev 2004;56:185–229.
[12] Rayman MP. The importance of selenium to human health. Lancet 2000;356:233–41.
[13] Tinggi U. Selenium: its role as antioxidant in human health. Environ Health Prev Med 2008;13:102–8.
[14] Papp LV, Holmgren A, Khanna KK. Selenium and selenoproteins in health and disease. Antioxidants Redox Signal 2010;12:793–5.
[15] Saygin M, Caliskan S, Ozguner MF, Gumral N, Comlekci S, Karahan N. Impact of L-carnitine and selenium treatment on testicular apoptosis in rats exposed to 2.45 GHz microwave energy. West Indian Med J 2015;64:55–61.
[16] Erkekoglu P, Zeybek ND, Giray B, Asan E, Hincal F. The effects of di(2-ethylhexyl)phthalate exposure and selenium nutrition on sertoli cell vimentin structure and germ-cell apoptosis in rat testis. Arch Environ Contam Toxicol 2012;62:539–47.
[17] Wilson R, McKillop JH, Travers M, Smith J, Smith E, Thomson JA. The effects of antithyroid drugs on intercellular mediators. Acta Endocrinol (Copenh) 1990;122:605–9.
[18] Chiao YC, Cho WL, Wang PS. Inhibition of testosterone production by propylthiouracil in rat Leydig cells. Biol Reprod 2002;67:416–22.
[19] Krassas GE, Pontikides N. Male reproductive function in relation with thyroid alterations. Best Pract Res Clin Endocrinol Metabol 2004;18:183–95.
[20] Ben Ali R, Ben Othman A, Bokri K, Maghraoui S, Hajri A, Ben Akacha A, et al. Synthesis and evaluation of analgesic, behavioral effects and chronic toxicity of the new 3,5-diaminopyrazole and its precursor the thiocyanoacetamide. Biomed Pharmacother 2017;86:109–17.
[21] Boussada M, Ali RB, Said AB, Bokri K, Akacha AB, Dziri C, et al. Selenium and a newly synthesized Thiocyanoacetamide reduce Doxorubicin gonadotoxicity in male rat. Biomed Pharmacother 2017;89:1005–17.
[22] Rato L, Alves MG, Socorro S, Duarte AI, Cavaco JE, Oliveira PF. Metabolic regulation is important for spermatogenesis. Nat Rev Urol 2012;9:330–8.
[23] Griswold M, Mably E, Fritz IB. Stimulation by follicle stimulating hormone and dibutyryl cyclic AMP of incorporation of 3H-thymidine into nuclear DNA of cultured Sertoli cell-enriched preparations from immature rats. Curr Top Mol Endocrinol 1975;2:413–20.
[24] Hai Y, Hou J, Liu Y, Liu Y, Yang H, Li Z, et al. The roles and regulation of Sertoli cells in fate determinations of spermatogonial stem cells and spermatogenesis. Semin Cell Dev Biol 2014;29:66–75.
[25] Viswanatha Swamy AH, Wangikar U, Koti BC, Thippeswamy AH, Ronad PM, Manjula DV. Cardioprotective effect of ascorbic acid on doxorubicin-induced myocardial toxicity in rats. Indian J Pharmacol 2011;43:507–11.
[26] Gao S, Li H, Feng XJ, Li M, Liu ZP, Cai Y, et al. alpha-Enolase plays a catalytically independent role in doxorubicin-induced cardiomyocyte apoptosis and mitochondrial dysfunction. J Mol Cell Cardiol 2015;79:92–103.
[27] Cabral RE, Okada FK, Stumpp T, Vendramini V, Miraglia SM. Carnitine partially protects the rat testis against the late damage produced by doxorubicin administered during pre-puberty. Andrology 2014;2:931–42.
[28] Chao HH, Liu JC, Hong HJ, Lin JW, Chen CH, Cheng TH. L-carnitine reduces doxorubicin-induced apoptosis through a prostacyclin-mediated pathway in neonatal rat cardiomyocytes. Int J Cardiol 2011;146:145–52.
[29] Sadeghi-Aliabadi H, Minaiyan M, Dabestan A. Cytotoxic evaluation of doxorubicin in combination with simvastatin against human cancer cells. Res Pharm Sci 2010;5:127–33.
[30] Huigsloot M, Tijdens IB, Mulder GJ, van de Water B. Differential regulation of doxorubicin-induced mitochondrial dysfunction and apoptosis by Bcl-2 in mammary adenocarcinoma (MTLn3) cells. J Biol Chem 2002;277:35869–79.
[31] Rato L, Alves MG, Dias TR, Cavaco JE, Oliveira PF. Testicular metabolic reprogramming in neonatal streptozotocin-induced type 2 diabetic rats impairs glycolytic flux and promotes glycogen synthesis. J Diabetes Res 2015;2015:973142.
[32] Wang S, Konorev EA, Kotamraju S, Joseph J, Kalivendi S, Kalyanaraman B. Doxorubicin induces apoptosis in normal and tumor cells via distinctly different mechanisms. intermediacy of H(2)O(2)- and p53-dependent pathways. J Biol Chem 2004;279:25535–43.
[33] Brunelle JK, Letai A. Control of mitochondrial apoptosis by the Bcl-2 family. J Cell Sci 2009;122:437–41.
[34] Vodovotz Y, Kim PK, Bagci EZ, Ermentrout GB, Chow CC, Bahar I, et al. Inflammatory modulation of hepatocyte apoptosis by nitric oxide: in vivo, in vitro, and in silico studies. Curr Mol Med 2004;4:753–62.
[35] Ryter SW, Mizumura K, Choi AM. The impact of autophagy on cell death modalities. Int J Cell Biol 2014;2014:502676.
[36] Mathurin K, Beauchemin C, Lachaine J. Validation of A Global economic model to evaluate the cost-effectiveness of targeted treatments using companion diagnostics in advanced/metastatic cancer treatment using kras testing for cetuximab therapy in metastatic colorectal cancer. Value Health 2014;17:A559.
[37] Jemal A, Siegel R, Ward E, Hao Y, Xu J, Murray T, et al. Cancer statistics, 2008. CA A Cancer J Clin 2008;58:71–96.
[38] Ward E, DeSantis C, Robbins A, Kohler B, Jemal A. Childhood and adolescent cancer statistics, 2014. CA A Cancer J Clin 2014;64:83–103.
[39] Campos JR, Rosa ESAC. Cryopreservation and fertility: current and prospective possibilities for female cancer patients. ISRN Obstet Gynecol 2011;2011:350813.
[40] Gautier J, Munnier E, Paillard A, Herve K, Douziech-Eyrolles L, Souce M, et al. A pharmaceutical study of doxorubicin-loaded PEGylated nanoparticles for magnetic drug targeting. Int J Pharm 2012;423:16–25.
[41] Hagiuda J, Ishikawa H, Kaneko S, Okazaki M, Oya M, Nakagawa K. Follicle-stimulating hormone enhances recovery from low-dose doxorubicin-induced spermatogenic disorders in mice. J Assist Reprod Genet 2015;32:917–23.
[42] Boekelheide K. Mechanisms of toxic damage to spermatogenesis. J Natl Cancer Inst Monogr 2005:6–8.
[43] Yeh YC, Lai HC, Ting CT, Lee WL, Wang LC, Wang KY, et al. Protection by doxycycline against doxorubicin-induced oxidative stress and apoptosis in mouse testes. Biochem Pharmacol 2007;74:969–80.
[44] Xie L, Lin L, Tang Q, Li W, Huang T, Huo X, et al. Sertoli cell-mediated differentiation of male germ cell-like cells from human umbilical cord Wharton's jelly-derived mesenchymal stem cells in an in vitro co-culture system. Eur J Med Res 2015;20:9.
[45] Behre HM, Bergmann M, Simoni M, Tuttelmann F. Primary testicular failure. In: De Groot LJ, Chrousos G, Dungan K, Feingold KR, Grossman A, Hershman JM, et al., editors. Endotext; 2000. South Dartmouth (MA).
[46] Tomankova K, Polakova K, Pizova K, Binder S, Havrdova M, Kolarova M, et al. In vitro cytotoxicity analysis of doxorubicin-loaded/superparamagnetic iron oxide colloidal nanoassemblies on MCF7 and NIH3T3 cell lines. Int J Nanomed 2015;10:949–61.
[47] Holmgren G, Synnergren J, Bogestal Y, Ameen C, Akesson K, Holmgren S, et al. Identification of novel biomarkers for doxorubicin-induced toxicity in human cardiomyocytes derived from pluripotent stem cells. Toxicology 2015;328:102–11.
[48] Adegoke E, Wang X, Wang H, Wang C, Zhang H, Zhang G. Selenium (Na 2 SeO 3) upregulates expression of immune genes and blood–testis barrier constituent proteins of bovine sertoli cell in vitro. Biol Trace Elem Res 2018;185:332–43.
[49] Chan FK, Moriwaki K, De Rosa MJ. Detection of necrosis by release of lactate dehydrogenase activity. Methods Mol Biol 2013;979:65–70.
[50] Frantz MC, Wipf P. Mitochondria as a target in treatment. Environ Mol Mutagen 2010;51:462–75.
[51] Kroemer G, Galluzzi L, Brenner C. Mitochondrial membrane permeabilization in cell death. Physiol Rev 2007;87:99–163.
[52] Buondonno I, Gazzano E, Jean SR, Audrito V, Kopecka J, Fanelli M, et al. Mitochondria-Targeted doxorubicin: a new therapeutic strategy against doxorubicin-resistant osteosarcoma. Mol Cancer Ther 2016;15:2640–52.
[53] Kuznetsov AV, Margreiter R, Amberger A, Saks V, Grimm M. Changes in mitochondrial redox state, membrane potential and calcium precede mitochondrial dysfunction in doxorubicin-induced cell death. Biochim Biophys Acta 2011;1813:1144–52.
[54] Zhou YJ, Zhang SP, Liu CW, Cai YQ. The protection of selenium on ROS mediated-apoptosis by mitochondria dysfunction in cadmium-induced LLC-PK(1) cells. Toxicol In Vitro 2009;23:288–94.
[55] Mehta SL, Kumari S, Mendelev N, Li PA. Selenium preserves mitochondrial function, stimulates mitochondrial biogenesis, and reduces infarct volume after focal cerebral ischemia. BMC Neurosci 2012;13:79.
[56] Wang Y, Wu Y, Luo K, Liu Y, Zhou M, Yan S, et al. The protective effects of selenium on cadmium-induced oxidative stress and apoptosis via mitochondria pathway in mice kidney. Food Chem Toxicol 2013;58:61–7.
[57] Shi D, Liao S, Guo S, Li H, Yang M, Tang Z. Protective effects of selenium on aflatoxin B1-induced mitochondrial permeability transition, DNA damage, and histological alterations in duckling liver. Biol Trace Elem Res 2015;163:162–8.
[58] Starkov AA. The role of mitochondria in reactive oxygen species metabolism and signaling. Ann N Y Acad Sci 2008;1147:37–52.
[59] Bagkos G, Koufopoulos K, Piperi C. A new model for mitochondrial membrane potential production and storage. Med Hypotheses 2014;83:175–81.
[60] Starkov AA. An update on the role of mitochondrial alpha-ketoglutarate dehydrogenase in oxidative stress. Mol Cell Neurosci 2013;55:13–6.
[61] Asensio-Lopez MC, Soler F, Sanchez-Mas J, Pascual-Figal D, Fernandez-Belda F, Lax A. Early oxidative damage induced by doxorubicin: source of production, protection by GKT137831 and effect on Ca(2+) transporters in HL-1 cardiomyocytes. Arch Biochem Biophys 2016;594:26–36.

[62] Zhao X, Wang Y, Gao JJ, Yin JJ. Inhibited effects of veliparib combined doxorubicin for BEL-7404 proliferation of human liver cancer cell line. Asian Pac J Trop Med 2014;7:468–72.
[63] Wei T, Chen C, Liu J, Liu C, Posocco P, Liu X, et al. Anticancer drug nanomicelles formed by self-assembling amphiphilic dendrimer to combat cancer drug resistance. Proc Natl Acad Sci U S A 2015;112:2978–83.
[64] Guerriero G, Trocchia S, Abdel-Gawad FK, Ciarcia G. Roles of reactive oxygen species in the spermatogenesis regulation. Front Endocrinol 2014;5:56.
[65] Eom YW, Kim MA, Park SS, Goo MJ, Kwon HJ, Sohn S, et al. Two distinct modes of cell death induced by doxorubicin: apoptosis and cell death through mitotic catastrophe accompanied by senescence-like phenotype. Oncogene 2005;24:4765–77.
[66] Synowiec E, Hoser G, Bialkowska-Warzecha J, Pawlowska E, Skorski T, Blasiak J. Doxorubicin differentially induces apoptosis, expression of mitochondrial apoptosis-related genes, and mitochondrial potential in BCR-ABL1-expressing cells sensitive and resistant to imatinib. BioMed Res Int 2015;2015:673512.
[67] Koleini N, Kardami E. Autophagy and mitophagy in the context of doxorubicin-induced cardiotoxicity. Oncotarget 2017;8:46663–80.
[68] Perl A, Gergely Jr P, Nagy G, Koncz A, Banki K. Mitochondrial hyperpolarization: a checkpoint of T-cell life, death and autoimmunity. Trends Immunol 2004;25:360–7.
[69] Ly JD, Grubb DR, Lawen A. The mitochondrial membrane potential (deltapsi(m)) in apoptosis; an update. Apoptosis 2003;8:115–28.
[70] Gewirtz DA. A critical evaluation of the mechanisms of action proposed for the antitumor effects of the anthracycline antibiotics adriamycin and daunorubicin. Biochem Pharmacol 1999;57:727–41.
[71] Sharifi S, Barar J, Hejazi MS, Samadi N. Doxorubicin changes Bax/Bcl-xL ratio, caspase-8 and 9 in breast cancer cells. Adv Pharmaceut Bull 2015;5:351–9.
[72] Wang C, Youle RJ. The role of mitochondria in apoptosis*. Annu Rev Genet 2009;43:95–118.
[73] Manov I, Pollak Y, Broneshter R, Iancu TC. Inhibition of doxorubicin-induced autophagy in hepatocellular carcinoma Hep3B cells by sorafenib–the role of extracellular signal-regulated kinase counteraction. FEBS J 2011;278:3494–507.
[74] Jacobs H, Bast A, Peters GJ, van der Vijgh WJ, Haenen GR. The semisynthetic flavonoid monoHER sensitises human soft tissue sarcoma cells to doxorubicin-induced apoptosis via inhibition of nuclear factor-kappaB. Br J Canc 2011;104:437–40.
[75] Li S, Zhou Y, Dong Y, Ip C. Doxorubicin and selenium cooperatively induce fas signaling in the absence of Fas/Fas ligand interaction. Anticancer Res 2007;27:3075–82.
[76] Huang Y, He L, Liu W, Fan C, Zheng W, Wong YS, et al. Selective cellular uptake and induction of apoptosis of cancer-targeted selenium nanoparticles. Biomaterials 2013;34:7106–16.
[77] Menter DG, Sabichi AL, Lippman SM. Selenium effects on prostate cell growth. Cancer Epidemiol Biomark Prev 2000;9:1171–82.
[78] Zhu X, Guo K, Lu Y. Selenium effectively inhibits 1,2-dihydroxynaphthalene-induced apoptosis in human lens epithelial cells through activation of PI3-K/Akt pathway. Mol Vis 2011;17:2019–27.
[79] Yeo JE, Kang SK. Selenium effectively inhibits ROS-mediated apoptotic neural precursor cell death in vitro and in vivo in traumatic brain injury. Biochim Biophys Acta 2007;1772:1199–210.
[80] Xu X, Chen K, Kobayashi S, Timm D, Liang Q. Resveratrol attenuates doxorubicin-induced cardiomyocyte death via inhibition of p70 S6 kinase 1-mediated autophagy. J Pharmacol Exp Ther 2012;341:183–95.
[81] Sun CY, Dou S, Du JZ, Yang XZ, Li YP, Wang J. Doxorubicin conjugate of poly(ethylene glycol)-block-polyphosphoester for cancer therapy. Adv Healthc Mater 2014;3:261–72.
[82] Yonekawa T, Thorburn A. Autophagy and cell death. Essays Biochem 2013;55:105–17.
[83] Arico S, Petiot A, Bauvy C, Dubbelhuis PF, Meijer AJ, Codogno P, et al. The tumor suppressor PTEN positively regulates macroautophagy by inhibiting the phosphatidylinositol 3-kinase/protein kinase B pathway. J Biol Chem 2001;276:35243–6.
[84] Crighton D, Wilkinson S, O'Prey J, Syed N, Smith P, Harrison PR, et al. DRAM, a p53-induced modulator of autophagy, is critical for apoptosis. Cell 2006;126:121–34.
[85] Thorburn A. Apoptosis and autophagy: regulatory connections between two supposedly different processes. Apoptosis 2008;13:1–9.
[86] Zhang YY, Meng C, Zhang XM, Yuan CH, Wen MD, Chen Z, et al. Ophiopogonin D attenuates doxorubicin-induced autophagic cell death by relieving mitochondrial damage in vitro and in vivo. J Pharmacol Exp Ther 2015;352:166–74.
[87] Wu S, Zhu L, Yang J, Fan Z, Dong Y, Luan R, et al. Hydrogen-containing saline attenuates doxorubicin-induced heart failure in rats. Die Pharmazie 2014;69:633–6.
[88] Li DL, Wang ZV, Ding G, Tan W, Luo X, Criollo A, et al. Doxorubicin blocks cardiomyocyte autophagic flux by inhibiting lysosome acidification. Circulation 2016;133:1668–87.
[89] Tacar O, Indumathy S, Tan ML, Baindur-Hudson S, Friedhuber AM, Dass CR. Cardiomyocyte apoptosis vs autophagy with prolonged doxorubicin treatment: comparison with osteosarcoma cells. J Pharm Pharmacol 2015;67:231–43.
[90] Shimizu S, Kanaseki T, Mizushima N, Mizuta T, Arakawa-Kobayashi S, Thompson CB, et al. Role of Bcl-2 family proteins in a non-apoptotic programmed cell death dependent on autophagy genes. Nat Cell Biol 2004;6:1221–8.